Journal of Materials Chemistry A

Expeditious Synthesis of Covalent Organic Frameworks: A Review

Journal:	*Journal of Materials Chemistry A*
Manuscript ID	TA-REV-06-2020-005894.R1
Article Type:	Review Article
Date Submitted by the Author:	08-Jul-2020
Complete List of Authors:	Li, Xinle; Lawrence Berkeley Laboratory, The Molecular Foundry Yang, Chongqing; Lawrence Berkeley Laboratory, The Molecular Foundry Sun, Bing; China University of Geosciences Beijing, School of Science; Institute of Chemistry Chinese Academy of Sciences, Key Laboratory of Molecular Nanostructure and Nanotechnology and Beijing National Laboratory for Molecular Sciences Cai, Songliang; South China Normal University Guangzhou Higher Education Mega Center, School of Chemistry and Environment Chen, Ziman; Beijing University of Chemical Technology, Beijing Key Laboratory of Bioprocess, College of Life Science and Technology, Lv, Yongqin; Beijing University of Chemical Technology, College of Life Science and Technology Zhang, Jian; Lawrence Berkeley National Laboratory Liu, Yi; Lawrence Berkeley National Laboratory, The Molecular Foundry

REVIEW

Expeditious Synthesis of Covalent Organic Frameworks: A Review

Xinle Li, [a] Chongqing Yang, [a] Bing Sun, [b] Songliang Cai, [c] Ziman Chen, [d] Yongqin Lv, [d] Jian Zhang, [a] Yi Liu*[a]

Received 00th January 20xx,
Accepted 00th January 20xx

DOI: 10.1039/x0xx00000x

Covalent organic frameworks (COFs), a burgeoning class of crystalline porous materials constructed by covalently connecting organic building blocks, have garnered tremendous attention. The predominant solvothermal synthesis of COFs usually requires high temperature and long reaction times (three days or longer), which creates substantial obstacles for their accelerated discovery and exploration in practical applications. Hence, the expeditious synthesis of COFs without compromising their inherent properties is exceedingly appealing from the viewpoint of cost, time, and energy footprint. To overcome the sluggishness of synthesis, considerable efforts have been invested in the rapid synthesis of high-quality COFs through innovations in energy source, catalyst, solvent, monomer, nucleation, and workup activation, leading to a drastic reduction of reaction time from multiday to a few hours, and even to seconds in some cases. In this contribution, we provide a comprehensive overview of the advances in expediting the synthesis science of COFs. Though a nascent effort, six prevalent strategies have been identified for the rapid synthesis of COFs, which have led to intriguing applications in a diverse range of areas including gas adsorption, separation, heterogeneous catalysis, environmental remediation, and photodynamic therapy. We also outline the major challenges and perspectives on the future directions empowered by expeditious COFs synthesis.

Introduction

Covalent organic frameworks (COFs) represent an emerging class of crystalline porous materials entirely composed of light elements and connected by reversible covalent bonds in two and three-dimensions (2D and 3D). Since the first seminal work in 2005,[1] COFs have been at the forefront of solid-state polymeric materials owing to their periodic skeletons, ultralow densities, high surface areas, amenable topologies, and diverse functionalities. The unique set of structural features underpins their widespread applications such as gas storage and separation, heterogeneous catalysis, chemical sensing, ionic conduction, energy storage, and optoelectronics.[2-7] The synthesis of COFs is generally achieved by stitching organic building units together using dynamic covalent chemistry.[8] The thermodynamically reversible bond formation facilitates the crystallization of COFs via self-healing and error-correction, during which the structural defects are dynamically repaired. Among the developed synthetic approaches, solvothermal synthesis is the most adopted process which usually takes multiple days and even several months in the case of 3D COF single crystals.[9, 10] The long reaction times, as well as cumbersome procedures and high energy-consumption, create substantial hurdles in the explorations of functional COFs.

To alleviate these shortcomings and empower an expeditious synthesis of COFs, a deep insight into the underlying crystallization process is imperative. Among the few pioneering mechanistic investigations, Dichtel and co-workers demonstrated that the formation of imine-linked 2D COF took place through the initial rapid precipitation of an amorphous polymer, which gradually crystallized into more ordered frameworks over days under dynamic conditions.[11] This amorphous-to-crystalline transition underlines the importance of promoting imine exchange and allowing sufficient reaction time to correct structural errors. On the other hand, 2D COFs with weak π-π interlayer stacking interactions are prone to undergo structural changes in response to external stimuli, such as these solvent-responsive COFs.[12-15] To preserve the subtle interlayer interactions and safeguard 2D COFs from structural collapse during the activation process, Feriante *et al*. noted that an elegant control of the activation protocol can avoid pore collapse and thus expedite the COF synthesis.[16] In order to accelerate the COF formation, exquisite controls must be exerted on conditions that can affect the rate of error-correction during the crystallization and/or the activation during workup.

A great deal of research efforts has been directed to promoting the rate of error-correction during the COF synthesis and circumventing the structural collapse in the workup procedures. Notable synthetic advances have been accomplished in the following aspects (Scheme 1): 1) Exploring alternative energy sources such as microwave, ultrasound, mechanical agitation, light, and electron beam due to their capability of boosting crystallization rate versus classical thermal energy. 2) Developing new and efficient catalysts that can enhance the rate of dynamic covalent exchange and augment the error-correction rate during the crystallization. 3) Using solvents to modulate the crystal growth and error-correction rate. 4) Manipulating the monomer structures to promote the crystal growth by either minimizing structural errors or enhancing the reversibility of covalent linkages. 5) Adopting a heterogeneous nucleation approach to regulate the crystallization of COFs. 6) Deploying new

[a] The Molecular Foundry, Lawrence Berkeley National Laboratory, Berkeley, California 94720, United States
[b] School of Science, China University of Geosciences (Beijing), Beijing 100083, P.R. China
[c] School of Chemistry, South China Normal University, Guangzhou 510006, P.R. China
[d] Beijing Key Laboratory of Bioprocess, College of Life Science and Technology, Beijing University of Chemical Technology, Beijing 100029, P.R. China

activation methods to mitigate structural collapse during the workup process.

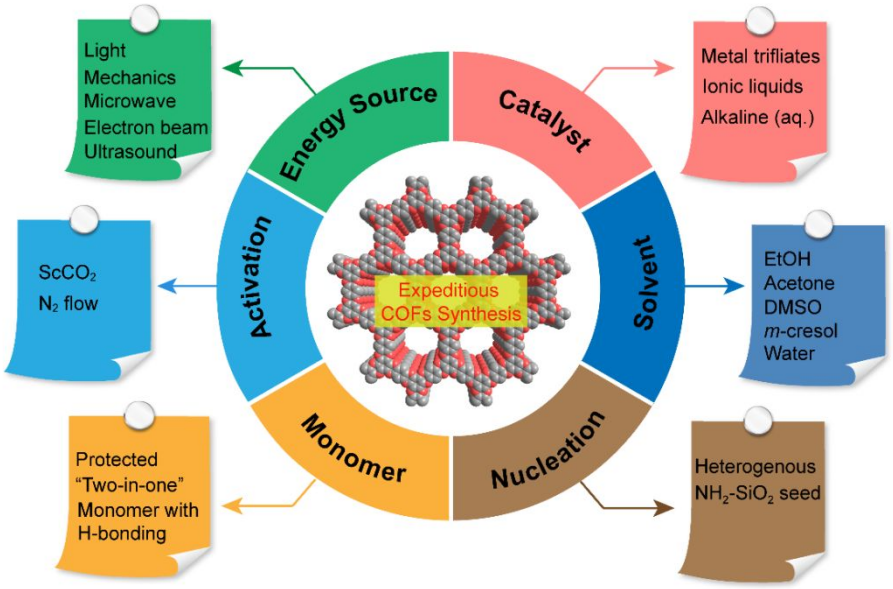

Scheme 1. Leading strategies for the expeditious synthesis of COFs through innovations in energy source, catalyst, solvent, monomer, nucleation, and workup activation.

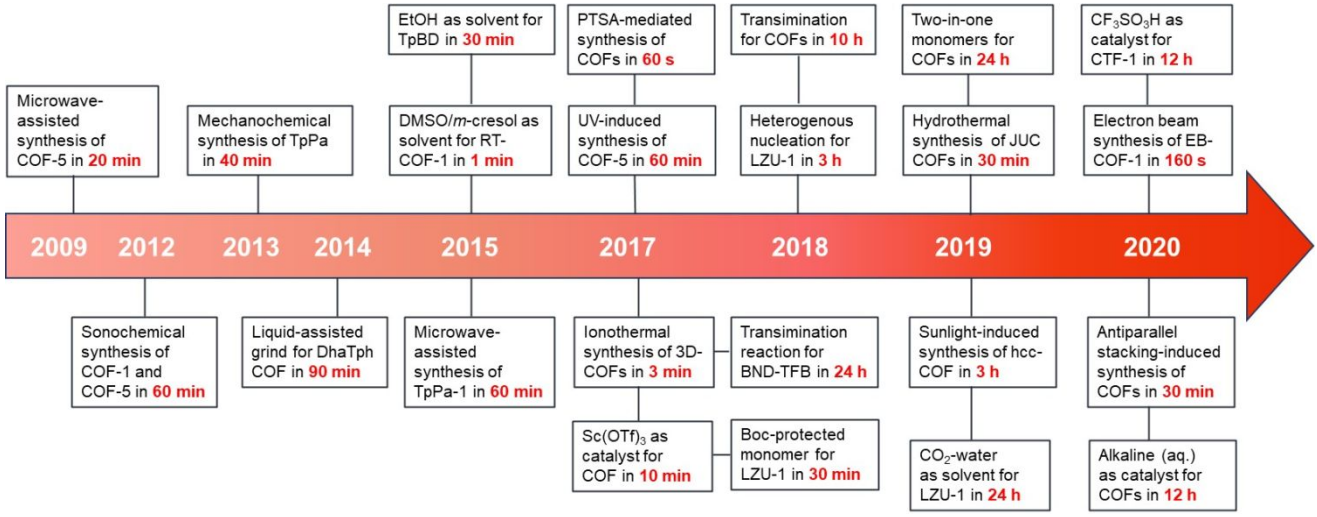

Scheme 2. Representative synthetic advances in the expeditious synthesis of bulk COFs.

In the past decade, considerable progress has flourished, leading to substantially shortened reaction times from multiday to several hours, and even seconds in extreme cases. Representative synthetic advances in the expeditious synthesis of bulk COFs have been depicted in Scheme 2. Despite a large number of COF reviews on the structural design,[17] synthetic strategies,[18] and specialized applications,[19-21] a timely and systematic review that encompasses the current progress regarding the rapid synthesis of COFs has not been conducted thus far and is much needed. Herein we discuss the mechanistic insights of 2D COF formation and the plausible rate-determining factors. Subsequently, we present an overview of the leading strategies for the expeditious synthesis of COFs. A summary of bulk COFs prepared within a short period of time from a minute to 24 hours by various methodologies is presented in Table 1 in reverse-chronological order. The diverse applications of expeditiously-synthesized COFs are also briefly discussed. Finally, we outline the challenges and future research directions for the expeditious synthesis of COFs.

Table 1. Summary of the representative examples of the rapid synthesis of bulk COFs.

COFs	Linkage	Synthetic Condition [a]	Scalable [b]	Time	BET Surface Areas	Strategy	Year	Reference
TAPB-PDA TAPB-OHPDA TAPB-OMePDA TAPPy-PDA TAPPy-NDI-DA	Imine	Mesitylene/1,4-dioxane AcOH, 70 °C	/	4 h	2890 m^2g^{-1} 950 m^2g^{-1} 2440 m^2g^{-1} 3140 m^2g^{-1} 1430 m^2g^{-1}	$ScCO_2$ activation	2020	16
THCOF (COF-318)	Aryl ether	Mesitylene/1,4-dioxane Triethylamine, 70 °C, MW	/	30 min	1254 m^2g^{-1}	Microwave synthesis	2020	45
EB-COF-1	Imine	DCB/*n*-BuOH AcOH, RT, electron beam	Yes	160 s	738 m^2g^{-1}	Electron beam irradiation	2020	37
COF-42-B	Hydrazone	Mesitylene/1,4-dioxane Stirring, $Sc(OTf)_3$, RT	/	30 min	367 m^2g^{-1}	New catalyst	2020	69
TzBA	Imine	Mesitylene/1,4-dioxane $Sc(OTf)_3$, 60 °C	/	24 h	156 m^2g^{-1}	New catalyst	2020	70
HP-TpAzo HP-TpPa HP-TpPa$(CH_3)_2$ HP-TpBD HP-COF-HNU1	Ketoenamine	$[C_4mim][BF_4]$ Stirring, 50 °C	/	12 h	179 m^2g^{-1} 727 m^2g^{-1} 298 m^2g^{-1} 467 m^2g^{-1} 475 m^2g^{-1}	New catalyst	2020	72
CTF-1 F-CTF-1 F-CTF-2	Triazine	CF_3SO_3H Solid-state, 250 °C	/	12 h	646 m^2g^{-1} 411 m^2g^{-1} 211 m^2g^{-1}	New catalyst	2020	78
TpPa-1 TpBD TpTph COF-NJU-1	Ketoenamine	KOH/DMF/H_2O Stirring, 140 °C	/	12 h	1247 m^2g^{-1} 768 m^2g^{-1} 658 m^2g^{-1} 1080 m^2g^{-1}	New catalyst	2020	82
MW TAPB-BTCA-COF	Imine	H_2O AcOH, 80 °C, MW	/	5 h	566 m^2g^{-1}	Microwave synthesis	2020	93
Tf-DHzOAll Tf-DHzOPrY Tf-DHzOBn	Hydrazone	DCB, AcOH String, 100-120 °C	Yes	30 min	701 m^2g^{-1} 501 m^2g^{-1} 254 m^2g^{-1}	Antiparallel stacking	2020	102
hcc-COF	Phenazine	Mesitylene/methanol AcOH, RT Simulated sunlight	/	3 h	598 m^2g^{-1}	Photochemical synthesis	2019	62
TAPB-PDA TAPB-BDA	Imine	CH_3CN $Sc(OTf)_3$, RT	/	20 h	2070 m^2g^{-1} N.D.	New catalyst	2019	68
TAPB-DMTP-COF	Imine	CH_3CN String, AcOH, RT	/	24 h	1000 m^2g^{-1}	New solvent	2019	86
LZU-1	Imine	AcOH CO_2/ H_2O, 4.5 MPa	/	24 h	678 m^2g^{-1}	New solvent	2019	89
HCOF-1	Azine	H_2O, 120 °C No catalyst	Yes	12 h	617 m^2g^{-1}	New solvent	2019	94
JUC-520 JUC-521 JUC-522 JUC-523	Ketoenamine	H_2O AcOH, RT	Yes	30 min	976 m^2g^{-1} 1127 m^2g^{-1} 1182m^2g^{-1} 1435 m^2g^{-1}	New solvent	2019	96
LZU-1	Imine	TFA, PVP, EtOH 120 °C	/	12 h	822 m^2g^{-1}	Boc-protected monomer	2019	98

Py-COF	Imine	AcOH Methylene chloride	/	24 h	1370 m^2g^{-1}	Two-in-one monomer	2019	99
COF-aminopyridine COF-$C_3H_7NH_2$	Ketoenamine	DMAc/DCB, AcOH Mono-functional amine 180 °C	Yes	10 h	1052m^2g^{-1} 1056 m^2g^{-1}	Imine exchange	2018	104
LZU-1	Imine	NH_2-SiO_2 AcOH, 120 °C	/	3 h	1571 m^2g^{-1}	Heterogenous nucleation	2018	107
COGF	Viologen	EtOH/H_2O Stirring, 100 °C, MW	/	2 h	N.D.	Microwave synthesis	2017	47
TpBa series	Ketoenamine	*p*-toluenesulfonic acid RT to 170 °C	Yes	1 min	538-3109 m^2g^{-1}	Mechanical synthesis	2017	58
UV-COF-5	Boronate ester	Mesitylene/1,4-dioxane RT, UV	/	60 min	2026 m^2g^{-1}	Photochemical synthesis	2017	36
TAPB-PDA TAPB-BPDA TAPB-TIDA	Imine	Mesitylene/1,4-dioxane $Sc(OTf)_3$, RT	/	10 min	2175 m^2g^{-1} 1235 m^2g^{-1} 692 m^2g^{-1}	New catalyst	2017	67
3D-IL-COF-1 3D-IL-COF-2 3D-IL-COF-3	Imine	[BMIm][NTf_2] RT	/	3 min	517 m^2g^{-1} 653 m^2g^{-1} 870 m^2g^{-1}	New catalyst	2017	71
sRT-COF-1	Imine	Acetone AcOH, string, RT	/	20 min	N.D.	New solvent	2017	85
LZU-1	Imine	TFA, PVP, EtOH 120 °C, MW	Yes	30 min	729 m^2g^{-1}	Boc-protected monomer	2017	97
BND-TFB TAPB-PDA DAB-TFP BND-TFP	Imine Ketoenamine	Mesitylene/1,4-dioxane AcOH, 120 °C	Yes	24 h	2314 m^2g^{-1} 1390 m^2g^{-1} 1277 m^2g^{-1} 1102 m^2g^{-1}	Imine exchange	2017	103
TpBpy-MC	Ketoenamine	Catalytic amounts of liquid Ball milling, RT	/	90 min	293 m^2g^{-1}	Liquid-assisted grinding	2016	57
TpPa-COF-MW	Ketoenamine	Mesitylene/1,4-dioxane AcOH, stirring, 120 °C MW	/	60 min	724 m^2g^{-1}	Microwave synthesis	2015	44
TpBD	Ketoenamine	EtOH, AcOH Stirring, RT	/	30 min	885 m^2g^{-1}	New solvent	2015	83
RT-COF-1	Imine	DMSO or *m*-cresol AcOH, string, RT	/	1 min	329 m^2g^{-1}	New solvent	2015	84
LZU-1 (LAG) DhaTph (LAG) TpTh (LAG)	Imine Ketoenamine Hydrazone	Catalytic amounts of liquid Ball milling, RT	/	90 min	N.D.	Liquid-assisted grinding	2014	56
BTD-COF	Boronate ester	Mesitylene/1,4-dioxane HCl, 180 °C, 10 min then 160 °C, 30 min MW	/	40 min	1000 m^2g^{-1}	Microwave synthesis	2013	43
TpPa-1 (MC) TpPa-2 (MC) TpBD (MC)	Ketoenamine	Solventless Grinding at RT	/	40 min	61 m^2g^{-1} 56 m^2g^{-1} 35 m^2g^{-1}	Mechanical synthesis	2013	35
COF-1 COF-5	Boronate ester	Mesitylene/1,4-dioxane 100 °C, sonication	Yes	60 min	732 m^2g^{-1} 2122 m^2g^{-1}	Sonochemical synthesis	2012	34

COF-5 (MW)	Boronate ester	Mesitylene/1,4-dioxane Stirring, 100 °C, MW	/	60 min	>2200 m^2g^{-1}	Microwave synthesis	2010	48
COF-5 COF-112	Boronate ester	Mesitylene/1,4-dioxane Stirring, 100 °C, MW	/	20 min	2019 m^2g^{-1} 2926 m^2g^{-1}	Microwave synthesis	2009	33

[a] MW: microwave. RT: room temperature. DCB: 1,2-dichlorobenzene. DMAc: dimethylacetamide. DMSO: dimethyl sulfoxide. TFA: trifluoroacetic acid. PVP: polyvinylpyrrolidone. [b] the assessment of scalability is based on whether it has been explicitly commented in the reference.

2. Mechanistic insights of COF formation

A clear elucidation of how COF crystals nucleate and grow is of paramount significance since it is the key to the rational design, synthesis, and improvement of new frameworks. Toward this end, a rigorous kinetic study of COF growth under reaction conditions can offer valuable mechanistic insight into its crystallization processes. To circumvent the typical heterogeneous reaction mixtures of COFs, Dichtel and co-workers designed homogenous growth conditions for the first mechanistic investigation of a prototypical boronate ester-linked COF (COF-5).[22] By virtue of kinetics studies wherein the reaction progression was determined by optical turbidity measurements, they found that COF-5 was formed rapidly without further improvements in its crystallinity afterward. Furthermore, the addition of competing monofunctional catechol decelerated the formation of COF-5 but did not disintegrate the existing COF, suggesting that the COF-5 formation involved a cascade reversible-irreversible transformation. Later in 2017, Dichtel, Bredas, and co-workers provided a theoretical insight into the crystallization process of COF-5.[23] They deployed a kinetic Monte Carlo (KMC) model to clarify the nucleation and growth of COF-5 from the homogenous conditions. The KMC simulations reproduced well with previously reported experimental growth kinetics. Another theoretical investigation to illuminate the crystallization of COF-5 was reported by Clancy's group in 2017.[24] By means of equilibrium path sampling (EPS), they calculated activation energies of three essential reactions that determine the initial nucleation of COF-5. Water and methanol were found to be essential to catalyze the boronate ester formation by lowering its activation energy barrier, in accordance with previous experimental observations. Furthermore, they ruled out a prior mechanism, i.e., polymerization of large sheets with subsequent stacking, and proposed a templated polymerization as a plausible growth mechanism for COF-5.

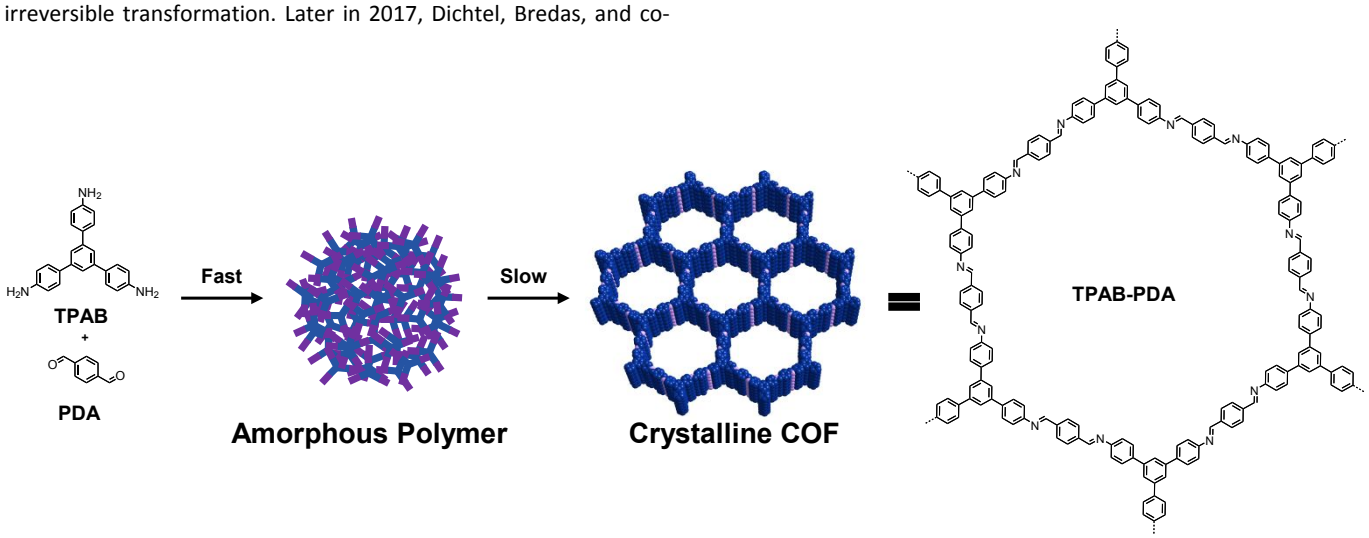

Fig. 1 Schematics of TAPB-PDA COF formation through an amorphous-to-crystalline transformation process.[11]

In marked contrast to boronate ester-linked COF-5, imine-linked 2D COF behaved differently in its crystallization process. Employing the 1,3,5-tris(4-aminophenyl)benzene (TAPB)/terephthalaldehyde (PDA) COF as a model system, Dichtel and co-workers revealed that the formation of imine-linked 2D COF (TAPB-PDA) underwent an amorphous-to-crystalline transformation process, wherein the initial rapidly-formed amorphous polymer (95% yield in just 15 minutes) crystallized into periodic frameworks over several days without the need of adding new COF precursors (Fig. 1).[11] Moreover, they elucidated the crucial role of acetic acid and water in inducing crystallinity and maintaining high yields in COFs formation. The amorphous-to-crystalline reconstruction has also been illustrated by Zhao, Zeng, and co-workers in the synthesis of other imine-linked COFs,[25] as well as by Liu and coworkers during the growth of LZU-COF thin films,[26] underscoring the vital roles of facile dynamic bonds exchange and adequate reaction time for COF growth. It is worth mentioning that such amorphous-to-crystalline transformation paves new avenues in the synthesis of crystalline COFs from amorphous polymers.[27-31] To date, mechanistic investigations on the nucleation and growth of COF are solely limited to boronate ester and imine-linked COFs. In light of the rapidly rising number of new linkages (over 20 in total),[32] an in-depth insight into the crystallization process of new COFs is a necessity.

3. Synthetic approaches for expeditious COF synthesis

3.1 New energy sources

The solvothermal synthesis of COFs relies on thermal energy to drive the reaction equilibrium towards thermodynamically stable crystalline products, which requires extended reaction time and high energy input. To mitigate such issues, alternative energy sources such as microwave,[33] ultrasound,[34] mechanical agitation,[35] light irradiation,[36] and electron beam[37] have been employed to expedite the nucleation of crystallites and thus enhance the overall synthetic rate of COFs.

3.1.1 Microwave-assisted solvothermal synthesis

Microwave-assisted synthesis has aroused enormous interest due to its unique attributes such as accelerated reaction rates, lower energy consumption, and higher yields.[38] Consequently, a wide array of functional materials including organic molecules,[39] metal oxides,[40] zeolites,[41] and metal-organic frameworks (MOFs)[42] have been prepared by microwave irradiation in an efficient, fast, and neat manner. In 2009, Cooper's group first reported the microwave-assisted synthesis of boronate ester-linked COFs (COF-5 and COF-102).[33] Under microwave irradiation at 100 °C, COF-5 was rapidly assembled via condensation of 1,4-benzenediboronic acid and 2,3,6,7,10,11-hexahydroxytriphenylene (HHTP) in 20 minutes both in sealed and open containers, which was 200 times faster than the classical solvothermal synthesis.[1] Remarkably, the resulting COF-5 exhibited higher Brunauer-Emmett-Teller (BET) surface areas (2019 $m^2\ g^{-1}$) than its solvothermal counterpart (1590 $m^2\ g^{-1}$) after removing trapped impurities in COF-5 through a potent microwave extraction process. In a similar manner, Bein's group demonstrated a rapid microwave-assisted synthesis of a mesoporous boronate ester-linked COF (BTD-COF).[43] Highly crystalline BTD-COF with a BET surface area of 1000 $m^2\ g^{-1}$ was prepared in 40 minutes under two consecutive microwave heating.

In addition to boron-based COFs, *β*-ketoenamine and dioxin-linked COFs have also been prepared rapidly by the microwave-assisted solvothermal method. In 2015, Wei's group first synthesized a *β*-ketoenamine-linked COF (TpPa-COF-MW) via the Schiff-base reaction of 1,3,5-triformylphloroglucinol (Tp) with *p*-phenylenediamine (Pa) under microwave irradiation for 1 hour.[44] As a comparison, conventional solvothermal synthesis without microwave irradiation only gave rise to a low yield of 8% in 1 hour. TpPa-COF-MW possessed excellent crystallinity and a higher BET surface area (724 $m^2\ g^{-1}$) than its solvothermal counterpart (535 $m^2\ g^{-1}$). It is noteworthy that TpPa-COF-MW showed exceptionally high CO_2 storage and high adsorption of CO_2 over N_2 at low pressures, placing itself as top CO_2 uptake material among reported COFs and other porous materials at the time. Most recently, Guo and co-workers extended this microwave-assisted strategy for the rapid synthesis of a dioxin-linked COF (THCOF) via aromatic nucleophilic substitution reaction between 2,3,5,6-tetrafluoro-4-pyridinecarbonitrile and HHTP in only 30 minutes,[45] which were considerably faster than the conventional solvothermal synthesis that took 72 hours. Crystalline THCOF showed an approximately 2-fold increase in the BET surface area (1254 $m^2\ g^{-1}$) compared to its solvothermal counterpart (576 $m^2\ g^{-1}$) reported previously.[46] When implemented as stationary coatings for solid-phase microextraction, THCOF exhibited efficient extraction of perfluorinated alkyl substances (PFASs) from aqueous medium and was highly reusable for 20 times without comprising its adsorptive performance, indicating the prospect of COFs adsorbents for water remediation. Despite that the reports on the microwave-assisted synthesis of COFs are comparatively limited, it has been proven in multiple cases that the microwave-assisted synthesis not only offers an expeditious alternative route to the conventional synthesis but also endows the obtained COFs with superior performance.[47, 48]

3.1.2 Sonochemical synthesis

Sonochemical synthesis is capable of accelerating the crystallization rate due to the acoustic cavitation in solutions, which engenders strikingly high local temperatures and pressures (>5000 K and >1000 bar) to realize ultrafast heating and cooling rates.[49] It also features low cost and energy consumption as it bypasses the induction period and requires a short synthesis time. In 2012, Ahn and co-workers first developed the sonochemical synthesis of boron-based COFs (COF-1 and COF-5) under ultrasonication for only 1 hour.[34] For instance, the resultant COF-5 exhibited a high BET surface area of 2122 $m^2\ g^{-1}$ and a 100-fold decrease in crystal sizes (~250 nm) relative to the conventional solvothermal counterpart. Moreover, sonochemical synthesis allowed for large-scale synthesis of COF-5 and displayed approximately 9 times higher space-time yield (the amount of product per volume of reaction mixture per day, 45 kg $m^{-3}\ day^{-1}$) than the COF analog synthesized under solvothermal conditions. The full potential of sonochemical synthesis is however yet to be unleashed as it has hitherto only been applied on boron-based COFs.

3.1.3 Mechanochemical synthesis

Mechanochemical (MC) synthesis has emerged as a viable route to the green synthesis of functional materials owing to its eco-friendliness, cost-effectiveness, and simplicity of operation.[50] A wide variety of porous materials such as porous carbons,[51] metal oxides,[52] graphene-derivatives,[53] and MOFs[54] have been prepared by means of MC synthesis. Nevertheless, the MC synthesis of COFs is still in its nascent stage and worth more earnest efforts.

In 2013, Banerjee's group first developed the solvent-free MC synthesis of COFs (TpPa-1(MC) and TpPa-2(MC)) by manually grinding the COF precursors in a mortar for 40 minutes at room temperature.[35] The resulting COFs showed moderate crystallinity, low BET surface area, and exceptional chemical stability in boiling water, 9 M HCl (aq.), and 3 M NaOH (aq.). In comparison to the solvothermal method, an extra benefit of MC synthesis is the spontaneous delamination of COFs to few-layered 2D nanosheets.[55] To fully harness the potential of MC synthesis, the same group developed in 2016 a liquid-assisted grinding (LAG) approach for the rapid synthesis of COFs (TpTh (LAG), DhaTph (LAG), and LZU-1 (LAG)).[56] Compared with the conventional MC method, LAG requires the addition of catalytic amounts of liquid to congregate reactants more closely and thereby enhance the yield and crystallinity of COFs. The LAG methodology allowed for the rapid synthesis of COFs bearing various linkages including *β*-ketoenamine, hydrazine, and imine in 90 minutes, much faster than the classical solvothermal synthesis. Employing LAG strategy, Banerjee and co-workers prepared a 2,2'-bipyridine-based COF (Tp-Bpy-MC) in 90 minutes at room temperature.[57] When utilized as a solid electrolyte in Proton Exchange Membrane fuel cells, Tp-Bpy-MC far surpassed its solvothermal analog with respect to open circuit voltage. Given the easiness of operation and nearly solventless process, this strategy is regarded as a competitive and viable synthetic route to the large-scale COF synthesis.

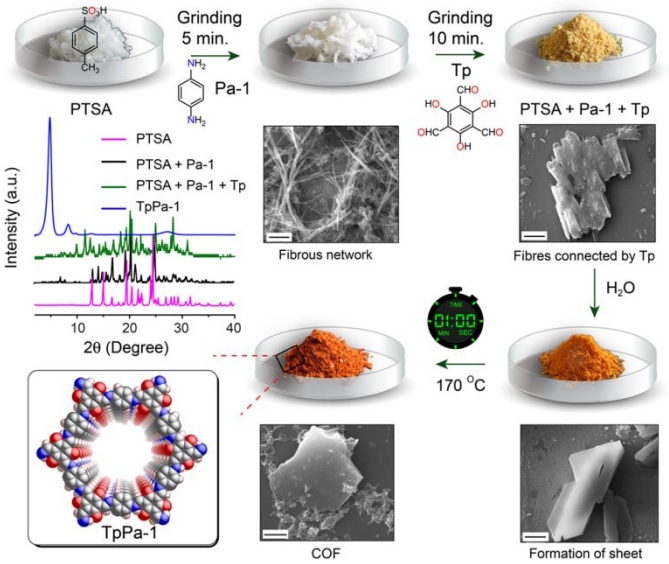

Fig. 2 MC synthesis of *β*-ketoenamine-linked COFs via a PTSA-mediated crystallization approach. Reproduced from ref. 58 with permission from the American Chemical Society, copyright 2017.

In 2017, Banerjee and co-workers reported a rapid and universal MC synthesis of *β*-ketoenamine-linked 2D COFs (12 in total) with the aid of *p*-toluenesulfonic acid monohydrate (PTSA·H_2O) (Fig. 2).[58] In a typical procedure, PTSA·H_2O and arylamine were mixed at first, then Tp was added into the mixture in the presence of water (~100 μL). After thorough grinding, the formed dough was heated at 170 °C for 60 seconds to flourish highly crystalline 2D COFs with extraordinarily high BET surface areas up to 3109 m^2 g^{-1}, the highest among the reported 2D COFs at the time. They attributed the rapid formation of COFs to the multiple roles of PTSA·H_2O, which served as a molecular organizer, water reservoir, and reactivity modulator in the MC synthesis of COFs. The facile protocol was amenable for the large-scale production of high-quality COFs (~10 g/h) using a twin-screw extruder and fabricating COFs with desired shapes. Notably, these molded COFs exhibited outstanding water adsorption that far exceeded the leading commercial zeolites, indicating the considerable appeal of COFs as solid dehumidifiers concerning their practical cost, exceptional performance, and simple regeneration. It is worth noting that MC synthesis of COFs has predominantly been demonstrated in the case of *β*-ketoenamine-linked 2D COFs until now, and it would be highly desirable to generalize its use in the synthesis of COFs with other intriguing linkages.

3.1.4 Photochemical synthesis

Photochemical synthesis has emerged as an efficient synthetic approach for diversified functional materials.[59-61] In 2017, Choi, Lim and co-workers reported the first photochemical synthesis of COF-5 (UV-COF-5) under UV irradiation at room temperature.[36] UV-COF-5 showed a 48-fold enhancement in the growth rate compared with the solvothermal counterpart. Furthermore, UV-COF-5 possessed uniform sea urchin-shape and ultrahigh BET surface area of 2027 m^2 g^{-1}. Notably, UV irradiation drastically enhanced the growth rate of UV-COF-5 along the [001] direction, presumably due to the UV-induced change in the interlayer orbital coupling, as supported by density functional theory (DFT) calculations. Most recently, Choi and co-workers implemented this photochemical synthetic strategy for the fast synthesis of pyrazine-fused COF (hcc-COF).[62] Under the irradiation of simulated sunlight (wavelength of 200-2500 nm) at room temperature, hcc-COF was constructed in just 3 hours via condensation of 1,2,4,5-benzenetetramine tetrahydrochloride and hexaketocyclohexane octahydrate. To highlight the essential role of light irradiation, the synthesis was carried out in the absence of light and only produced amorphous polymers. On account of its fully fused skeletons and structural regularity, the bulk electrical conductivity of hcc-COF pellet reached 2.22 × 10^{-3} S m^{-1}, which is among the highest values among the reported COFs.[63]

3.1.5 Electron beam irradiation-induced synthesis

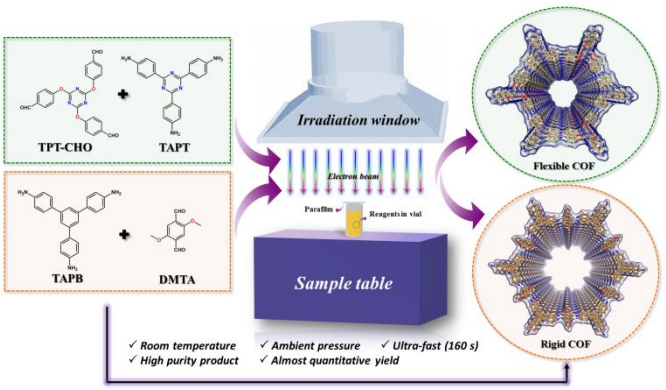

Fig. 3 Schematics of the experimental setup of the electron beam accelerator and electron beam-induced synthesis of COFs. Reproduced from ref. 37 with permission from the American Chemical Society, copyright 2020.

The past decade has witnessed the surge of high-energy ionizing radiations as energy sources for the synthesis of diverse functional materials.[64-66] Most recently, Wang's group developed an electron beam irradiation-induced synthesis of imine-linked 2D COFs with exceptional synthetic rates and generality (Fig. 3).[37] An imine-linked COF (EB-COF-1) bearing flexible skeletons was assembled in just 160 seconds via condensation between 2,4,6-tris-(4-formylphenoxy)-1,3,5-triazine and TAPB under high-energy electron beam (1.5 MeV) irradiation at room temperature. EB-COF-1 displayed a comparable BET surface area of 738 m^2 g^{-1} relative to its solvothermal counterpart. It was reasoned that the electron beam irradiation quickly "froze" the most stable conformation of EB-COF-1 and thus led to an enhanced crystallinity superior to its solvothermal analog. This electron beam-induced synthetic methodology is highly universal, as being demonstrated in the rapid synthesis of reported COFs and one new COF that was inaccessible via the conventional solvothermal approach (24 COFs in total). The ultrafast synthetic rate, together with the drastically diminished energy consumption, renders electron beam-induced synthesis a potent approach for the industrial production of COFs and opens up a new route to COFs that are hard to prepare otherwise.

3.2 New catalysts

Catalyst is capable of accelerating an organic reaction by lowering the activation energy. Developing high-performance catalysts to expedite the reactions toward desired products has been a long-sought-after goal in catalysis and materials discovery. Aqueous acetic acid (AcOH) is the most commonly used catalyst in the solvothermal synthesis of imine-linked COFs, which typically requires undesirable long reaction times and elevated temperatures.

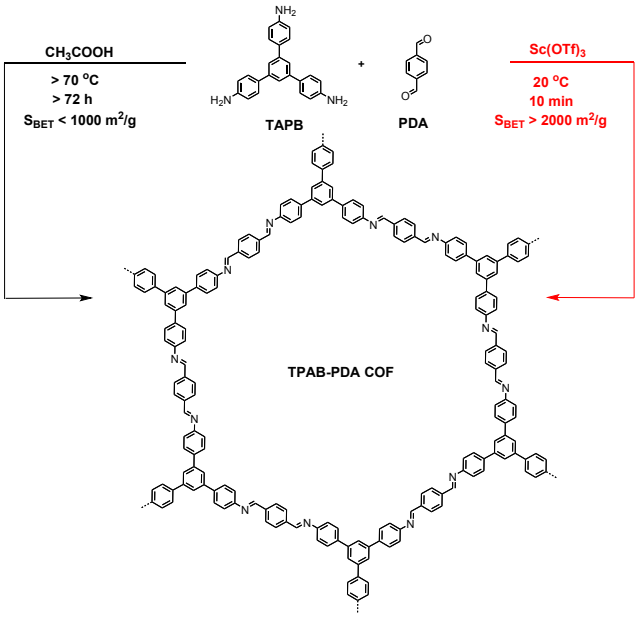

Fig. 4 Schematics of the synthesis of TAPB-PDA COF using conventional acetic acid-catalyzed (left) and new Lewis acid-catalyzed conditions.

In light of the crucial role of catalyst in COFs formation, Dichtel's group first employed a new and efficient catalyst, metal triflate, for the rapid synthesis of imine-linked 2D COFs in 2017 (Fig. 4).[67] Scandium triflate ($Sc(OTf)_3$) drastically shortened the synthesis time of COFs from multiday to only 10 minutes at room temperature. As a comparison, no precipitation was formed after two weeks at 90 °C when an equimolar amount (0.02 equiv) of AcOH was used as a catalyst. Moreover, the resultant COFs showed an ultrahigh BET surface area of 2175 $m^2 g^{-1}$, which far exceeded the reported TAPB-PDA COF (~600 $m^2 g^{-1}$) using AcOH-catalyzed conditions. In a subsequent study in 2019, the same group demonstrated a rapid synthesis of colloidal imine-linked COF nanoparticles using $Sc(OTf)_3$ in acetonitrile solvent.[68] The highly uniform spherical COF colloids were obtained within 20 hours and displayed superb crystallinity and high BET surface areas. *In situ* X-ray scattering experiments further indicated an amorphous-to-crystalline transition, which was in line with prior mechanistic studies of imine-linked COFs. Most recently, Chen and co-workers deployed a sacrificial templating approach to fabricate hollow COF capsules for enzyme immobilization.[69] A hydrazone-linked COF shell (COF-42-B) around enzyme-embedded MOF core was formed in only 30 minutes catalyzed by $Sc(OTf)_3$ at room temperature. After etching the MOF core with phosphate buffer solution (pH = 5), the hollow COF-42-B capsule was produced with enzyme encapsulated inside the cavity. The COF capsule could function as an efficient bioreactor with preserved enzymatic conformation and activity. The rational selection of $Sc(OTf)_3$ as the catalyst not only empowered the rapid synthesis of COFs under mild conditions,[70] but also circumvented the deconstruction of the fragile enzyme@MOF systems.

Beyond 2D COFs, Fang's group first utilized ionic liquids (ILs) as both catalyst and solvent for the room-temperature synthesis of 3D COFs (3D-IL-COFs).[71] The ionothermal synthesis resulted in an ultrafast formation of imine-linked 3D COF within minutes in an open vessel, significantly faster than their solvothermal counterparts acquired in sealed tubes for 72 hours at elevated temperature. Notably, ILs could be facilely recycled three times without impacting the synthesis. The resulting 3D-IL-COFs showed high separation efficiency for CO_2/N_2 and CO_2/CH_4 at room temperature. Analogously, Wang and co-workers lately employed ILs as catalyst/solvent for the rapid synthesis of hierarchically porous 2D COFs (HP-TpPa, HP-TpPa $(CH_3)_2$, HP-TpBD, and HP-COF-HNU1) in 12 hours,[72] which was 5 times faster than the AcOH-catalyzed solvothermal synthesis. The obtained HP-COFs were highly crystalline, chemically robust, and their hierarchical pores can be well controlled by altering the length of alkyl chains in ILs. Compared with the mono-pore COFs acquired by the solvothermal approach, HP-COFs displayed superior catalytic activity, especially for the bulky molecules-based Suzuki reaction.

Covalent triazine frameworks (CTFs) bearing aromatic triazine linkages and conjugated skeletons have been extensively studied due to their exclusive structural features compared to conventional COFs.[73] The synthesis of CTFs typically requires long reaction times (72 hours), high temperature (> 400 °C), and excess usage of catalysts due to much lower reversibility of triazine linkages.[74-77] To tackle these challenges, Dai's group deployed organic superacids as new catalysts for the rapid solid-state synthesis of crystalline CTFs.[78] The trimerization of 1,4-dicyanobenzene catalyzed by CF_3SO_3H (0.5 equiv) at 250 °C produced CTF-1 adopting a staggered stacking mode in only 12 hours. The resulting framework was further thermally annealed to yield CTF-1 with an eclipsed stacking mode while retaining its high crystallinity and porosity. Upon switching the stacking mode, CTF-1 presented an obvious color change from orange to greenish. Furthermore, this strategy is applicable to the preparation of crystalline fluorinated CTFs (F-CTF-1 and F-CTF-2) with adjustable fluorine content via a mixed-linker strategy.

Lewis or Brønsted acids are predominant catalysts for nitrogen-based COF (e.g., imine, azine, hydrazone, imide-linked COF) synthesis while bases have been rarely explored.[79-81] Most recently, Huang's group utilized aqueous alkaline hydroxides (MOH, M = Na, K, and Cs) as catalysts for the rapid synthesis of *β*-ketoenamine-linked COFs (COF-NJU-1, TpPa-1, TpBD, and TpTph).[82] Taking COF-NJU-1 as an example, by refluxing tetraaldehyde and benzidine in diethylformamide (DEF)/H_2O with KOH under stirring for 24 hours, COF-NJU-1 was readily synthesized with high crystallinity and BET surface area of 1080 $m^2 g^{-1}$. To manifest the generality of the basic hydrothermal approach, they prepared three *β*-ketoenamine-linked 2D COFs (TpPa-1, TpBD, and TpTph) under DMF/H_2O/KOH conditions in 24 hours, significantly faster than their solvothermal counterparts prepared via the AcOH-catalyzed synthesis (72 hours). It was postulated that aqueous alkali hydroxide decelerated the imine condensation and thereby fostered the crystallization of COFs. This basic hydrothermal approach offers a facile, rapid, green, and scaleup route to the synthesis of COFs, and the underlying crystallization mechanism is worth further research efforts.

3.3 New solvents

COFs formation via solvothermal synthesis is rather sensitive to the selection of solvents, which profoundly influences the crystallization rate and quality of COFs. Solvent screening is typically perceived as the rate-determining step in the tedious COF synthesis. As a consequence, selecting suitable solvents is essential for the expeditious solvothermal synthesis of COFs.

Instead of using the conventional solvents such as mesitylene and dioxane, Yan's group first deployed ethanol in 2015 for the rapid synthesis of a *β*-ketoenamine-linked COF (TpBD) within 30 minutes at room temperature.[83] Notably, TpBD exhibited a much higher BET surface area of 885 $m^2 g^{-1}$ than its solvothermal counterpart (537 $m^2 g^{-1}$) and mechanochemically synthesized analog (35 $m^2 g^{-1}$). When employed as the stationary phase for high-resolution gas chromatography, the TpBD-coated capillary column showed a faster

baseline separation of industrial analytes than the commercial HP-5 capillary column. Along this line, Zamora, Maspoch, and co-workers utilized DMSO or *m*-cresol for the ultrafast synthesis of an imine-linked COF (RT-COF-1) at room temperature in just 1 minute.[84] RT-COF-1 can be further fabricated on solid surfaces and flexible supports by means of soft-lithography and ink-jet printing, respectively. Subsequently, the same group selected acetone as a new solvent for the synthesis of s-RT-COF-1 in only 20 minutes.[85] Interestingly, s-RT-COF-1 adopted spherical morphologies with a uniform diameter of ~600 nm, in spite of inferior crystallinity and porosity. These studies clearly imply that beyond reaction rate, solvent renders an elegant control over the size, morphology, and processability of 2D COFs.[86] Inspired by this, Ma *et al*. recently developed a room-temperature synthesis of spherical imine-linked COFs in acetonitrile, wherein COF particle sizes were well controlled by simply altering the amount of acidic catalyst.[87]

In contrast to organic solvents, compressed CO_2 is an attractive alternative due to its benign, low-cost, nonflammable, and reusable nature.[88] In 2018, Zhang's group utilized CO_2-dissolved water as the solvent for the rapid synthesis of imine-linked COF (COF-LZU-1) at room temperature. COF-LZU-1 was assembled within 24 hours via condensation of 1,3,5-triformyl benzene and *p*-phenylenediamine in the CO_2/water medium.[89] COF-LZU-1 showed high crystallinity and superior surface area (678 m^2 g^{-1}) against its solvothermal counterpart synthesized in organic solvents (410 m^2 g^{-1}).[90] The high crystallinity, porosity, and nitrogen-rich skeletons conferred COF great potential as promising supports for metal nanoparticles. Palladium (Pd) nanoparticles with an average size of 2 nm were immobilized in COF-LZU-1, and the resultant Pd/COF-LZU-1 hybrid composite displayed high activity, selectivity, and recyclability in the hydrogenation of phenylacetylene, far surpassing the performance of the commercial Pd/carbon catalyst. Moreover, this facile approach also enabled the *in-situ* synthesis of gold and copper nanoparticles in COFs at room temperature.

Water is deemed as an environmentally benign solvent, and hydrothermal synthesis has been widely exploited in the preparation of various functional materials including COFs.[80, 91-93] In 2019, Zhao's group employed water as the sole solvent for the catalyst-free and scaleup synthesis of azine-linked COFs (HCOF-1-3) within several hours,[94] which was significantly faster than the solvothermal protocol in organic solvents.[95] A 10-gram scale synthesis of HCOF-1 was achieved in 12 hours via condensation of Tp and hydrazine in water without any catalysts. The resultant HCOF-1 exhibited high crystallinity and improved BET surface area of 617 m^2 g^{-1} relative to its solvothermal analogs (415-512 m^2 g^{-1}) synthesized in organic solvents. Furthermore, when exploited as column stuffing for organic dye separations, HCOF-1 displayed high adsorption of positively charged dye (methylene blue) while poor adsorption of the negatively charged ones (methylene orange and AR1).

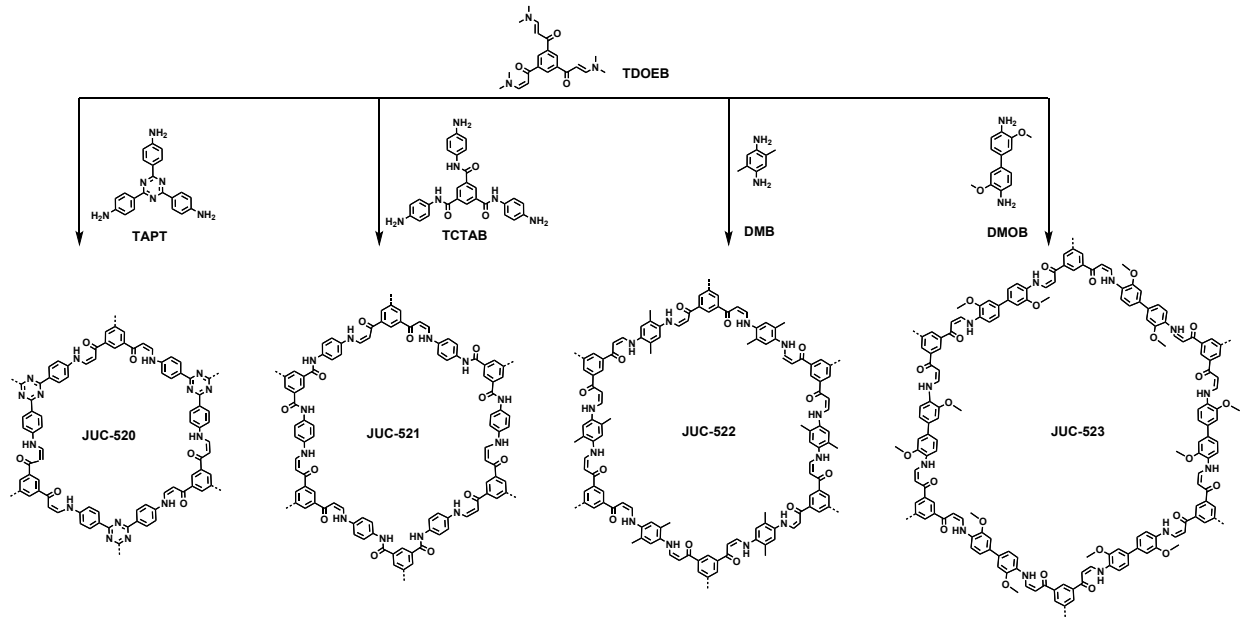

Fig. 5 The rapid aqueous synthesis of *β*-ketoenamine-linked COFs, JUC-520, JUC-521, JUC-522, and JUC-523 with varied pore sizes.

The hydrothermal protocol is also amenable to the fast construction of *β*-ketoenamine-linked COFs. Fang's group reported in 2019 the rapid aqueous synthesis of *β*-ketoenamine-linked COFs (JUC-520-523) by Michael addition-elimination reactions (Fig. 5).[96] A series of JUC COFs with varied pore sizes were synthesized at room temperature in only 30 minutes and high yields. In addition to ultrahigh reaction rates, JUC COFs showed excellent crystallinity and BET surface areas (976 m^2 g^{-1} to 1435 m^2 g^{-1}). Importantly, this hydrothermal approach enabled the 5-gram scale production of high-quality COFs within a short reaction time. Thanks to the chemical robustness and porous nature of COFs, Fe (II) was facilely immobilized in JUC-COFs and the resulting Fe-COF composite showed remarkable catalytic performance in the oxidative degradation of organic pollutants in aqueous solution. For instance, JUC-521-Fe efficiently catalyzed the degradation of noxious rhodamine 6G dye, significantly outperforming the classical TiO_2-based composites. This study opens up a promising avenue to the industrial synthesis of COFs and uncovers their enormous potential in environmental remediation.

3.4 New monomers

3.4.1 Protected amine monomers

Nucleation and crystal growth are two essential steps during COF formation. Accordingly, control over nucleation significantly impacts the synthetic rate of COFs. Such control is, however, often

complicated by the heterogenous amorphous precipitates in the COFs synthesis. To overcome such a challenge, Zhao *et al.* developed in 2017 a homogeneous synthetic route to imine-linked COFs wherein crystallization starts from homogeneous solutions rather than amorphous precipitates.[97] Instead of using traditional *p*-phenylenediamine, they utilized singly *tert*-butyloxycarbonyl (Boc) protected amine (NBPDA) as a new building block, which was deprotected *in situ* to amine and thereby facilitated the crystallization of COFs. Using this new monomer, they prepared LZU-1 COF in only 30 minutes via Schiff-base condensation of NBPDA and 1,3,5-triformyl benzene under microwave irradiation with PVP as the capping agent. The resulting LZU-1 displayed a dramatically higher BET surface area of 729 m^2 g^{-1} than that prepared via the conventional approach (410 m^2 g^{-1}).[90] In addition, this methodology is applicable to two other imine-linked COFs with diversified structures. Analogously, Dong and co-workers constructed in 2019 LZU-1 using NBPDA without the microwave irradiation in 12 hours. Subsequently, the photosensitizer, boron-dipyrromethene (BODIPY), was covalently attached to LZU-1 via condensation between the defective aldehyde sites in COF and the amino-tagged BODIPY.[98] The resulting BODIPY containing nanoscale COF (LZU-1-BODIPY) was exploited for the first time as photodynamic therapeutic agents, and it displayed low dark toxicity and pronounced phototoxicity in *in vitro* and *in vivo* studies, revealing the potential of COFs as nanomedicines for cancer therapeutics.

3.4.2 "Two-in-one" bifunctional monomers

Solvothermal synthesis of COFs mostly relies on laborious trial-and-error procedures to optimize reaction parameters. Hence, a molecular design strategy that simplifies the tedious procedures in COF synthesis is highly appealing. In 2019, Chen's group reported a unique "two-in-one" strategy for the rapid synthesis of imine-linked 2D COFs.[99] Contrasting with traditional monomers, they designed a bifunctional building block, 1,6-bis(4-formylphenyl)-3,8-bis(4-aminophenyl) pyrene (BFBAPy), by incorporating two distinct functional groups, i.e., amino and formyl groups, in one pyrene molecule. Remarkably, the self-condensation of BFBAPy gave rise to a highly crystalline Py-COF in a wide array of common organic solvents, attesting to a rare solvent adaptability in COF synthesis. This "two-in-one" strategy enables the rapid synthesis of Py-COF within 24 hours in as many as 11 different solvents, which greatly simplified the synthetic procedure and expedited the COFs synthesis by circumventing the tedious solvent screening.

3.4.3 Monomers with bond dipole moments and spatial orientations

Since the first report in 2011,[100] hydrazone-linked COFs are recognized as potential candidates for industrial production due to the facile synthesis of hydrazide building blocks. However, hydrazone-linked COFs are still quite limited and require multiday synthetic time.[101] Developing new and high-quality hydrazine-linked COFs in a fast manner is currently of significant interest.

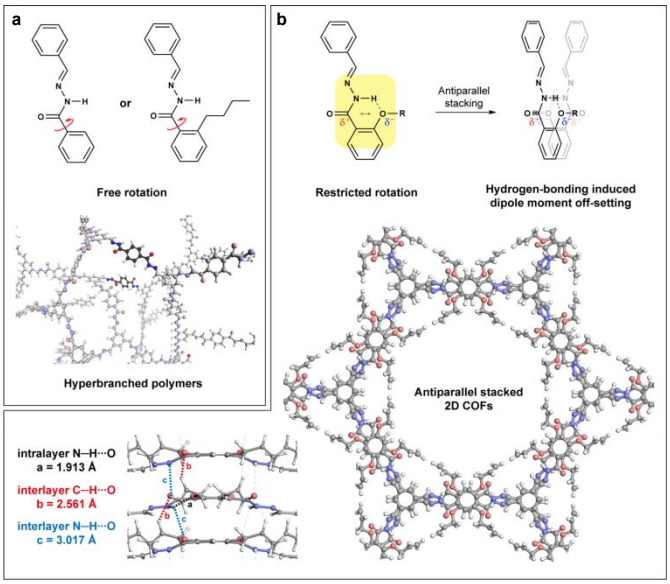

Fig. 6 Ultrafast synthesis of highly crystalline COFs via dipole-induced antiparallel stacking. (a) Formation of amorphous polymers from rotationally unrestricted building units. (b) COF formation via rotationally regulated synthesis. Reproduced from ref. 102 with permission from the American Chemical Society, copyright 2020.

Given that the error-correction process is the rate-determining step in COFs synthesis, minimizing structural errors that originate from random interlayer stacking and free intramolecular bond rotation is anticipated to expedite the COF formation. Toward this end, Loh's group demonstrated an ultrafast synthesis of hydrazone-linked COFs by using monomers that facilitate the antiparallel stacking in COF layers (Fig. 6).[102] They synthesized a number of monomers, 2,5-dialkyloxylterephthalohydrazides (DHzOR, R = allyl, propyl, and benzyl) that featured both in-plane rigidity and out-of-plane flexibility. Using DHzOR as building blocks, they constructed a series of hydrazone-linked COFs in just 30 minutes and gram-scale (up to 1.4 g). The highly crystalline COFs showed adequate BET surface areas comparable to those synthesized with longer times. This ultrafast synthesis of high-quality COFs was attributed to inter/intramolecular hydrogen bonding that favors the antiparallel stacking of COFs, which were supported by DFT calculations as well. Notably, the generalizable methodology allows for the rapid and scalable synthesis of hydrazone-linked COFs with variable geometries and functionalities. The rational design of the monomer structures to minimize structural errors paves a new way to the rapid and large-scale production of hydrazine-linked COFs.

3.4.4 Imine monomers for tranimination

N-aryl benzophenone imines have emerged as superior alternatives for unprotected amines due to their enhanced solubility, oxidative robustness, and easy preparation. More importantly, *N*-aryl benzophenone imines enable COFs growth via dynamic imine exchange reactions other than direct imine condensations, which might improve the inherent properties (e.g., crystallinity and porosity) of COFs.

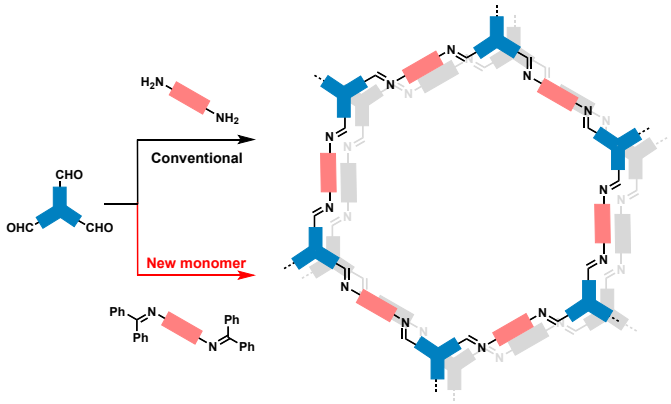

Fig. 7 Synthesis of imine-linked 2D COFs from conventional aryl amine monomers (upper) and new *N*-aryl benzophenone imines (bottom).

In 2017, Dichtel's group utilized *N*-aryl benzophenone imines as new building blocks for the rapid synthesis of nitrogen-linked COFs (i.e., imine and *β*-ketoenamine-linked COFs) with superb generality and scalability (Fig. 7).[103] 2D COFs were synthesized within 24 hours with high crystallinity and significantly enhanced BET surface areas in comparison to those synthesized using aryl amine monomers. This approach is also applicable to microwave-assisted synthesis and enables the synthesis of high-quality COFs in a much shorter time of 5 hours. It was postulated that the slow *in-situ* deprotection of *N*-aryl benzophenone imines controlled the number of unprotected amines and thereby improved the growth of COFs. Likewise, Liu and co-workers developed a rapid and scalable synthesis of imine-linked 2D COFs through dynamic imine exchange reactions.[104] Unlike the conventional aldimine condensation, the formyl linker, Tp, was initially reacted with a truncated amine monomer (e.g., *n*-propylamine) to yield imines, which subsequently crosslinked with benzidine through an imine exchange reaction. Highly crystalline COFs were expeditiously produced in only 6 hours in a flask in lieu of the commonly used sealed vessels. The resulting COF showed substantially improved BET surface area (1056 $m^2 g^{-1}$) relative to the conventional solvothermal counterpart (537 $m^2 g^{-1}$). In addition, COF nanofibers were uniformly grown on the polyimide films and the resulting COF-polyimide hybrid revealed a reversible colorimetric behavior upon exposure to acid vapors.

3.5 Heterogeneous nucleation

Fig. 8 Schematics of the rapid synthesis of LZU-1 COF through a heterogeneous nucleation and growth approach. Adapted from ref. 108 with permission from Springer, copyright 2017.

The dominant crystallization pathway of imine-linked 2D COFs involves the early immediate formation of amorphous networks that serve as heterogeneous sites for nucleation, with the subsequent amorphous-to-crystalline transition.[11] Such heterogeneous nucleation has been previously exploited in the synthesis of zeolites[105] and MOFs.[106] In 2018, Wang's group applied the heterogeneous nucleation strategy in the rapid synthesis of LZU-1 COF within 3 hours (Fig. 8).[107] To implement heterogeneous nucleation and growth approach, they initially assembled amorphous polyimine on the surface of an amino-functionalized SiO_2 (NH_2-SiO_2) as seeds. Subsequently, COF precursors were charged into the seeds solution to grow crystalline LZU-1 onto NH_2-SiO_2. After etching SiO_2 core with HF solutions, hollow COF was readily achieved with high crystallinity and substantially enhanced BET surface area (1571 $m^2 g^{-1}$) compared with the conventional solvothermal analog (410 $m^2 g^{-1}$). The authors postulated that the heterogeneous nuclei decelerated the rapid precipitation of kinetic amorphous networks and thereby facilitated the crystallization of COFs.[108]

3.6 Different activation methods

Upon completion of synthesis, COFs are usually washed with copious organic solvents to remove the trapped impurities, followed by vacuum drying at elevated temperatures. This widely-used workup procedure could be problematic because of the possible distortions of layered COFs during vacuum activation, thus undermining their crystallinity and porosity. To circumvent the structural collapse during vacuum activation, supercritical carbon dioxide ($scCO_2$) treatment is usually adopted as an alternative and non-destructive technique for activating porous materials without provoking significant capillary forces.[109]

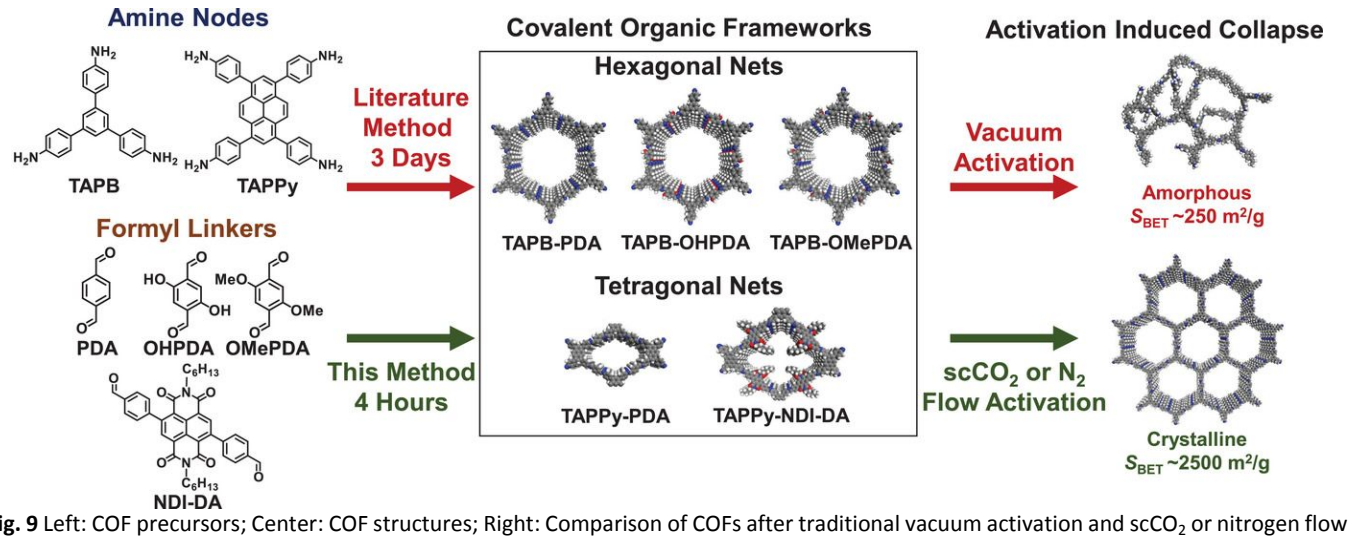

Fig. 9 Left: COF precursors; Center: COF structures; Right: Comparison of COFs after traditional vacuum activation and $scCO_2$ or nitrogen flow activation, respectively. Reproduced from ref. 16 with permission from the Wiley, copyright 2020.

Most recently, Feriante *et al*. demonstrated that, by avoiding pore collapse during the activation, facile and rapid synthesis of imine-linked 2D COFs could be achieved in just 4 hours (Fig. 9), which were much faster than the previous synthesis that took multiday reaction times.[16] Specifically, imine-linked COFs were acquired within several hours under solvothermal conditions and subjected to $scCO_2$ activation or by solvent exchange and subsequent drying under nitrogen flow. They investigated the effect of the activation procedure on a prototypical TAPB-PDA COF that was most likely to undergo pore collapse during the conventional vacuum activation. Upon appropriate activation with $scCO_2$, five imine-linked 2D COFs (TAPB-PDA, TAPB-OHPDA, TAPB-OMe-PDA, TAPPy-PDA, and TAPPy-NDI-DA) were expeditiously formed in 4 hours with excellent crystallinity and high BET surface areas, including record-high surface areas for three COFs reported thus far. This new workup protocol is expected to accelerate the discovery and exploration of new COFs, particularly these sensitive to vacuum activation.

4. Conclusion and future prospect

The expeditious synthesis of COFs has garnered increasing attention and has been actively explored in the past decade, which undoubtedly improves the long-term prospects of COFs. In this article, we have presented a comprehensive overview of the expeditious synthesis of high-quality COFs without compromising their inherent properties. We further summarized six leading synthetic strategies concerning energy source, catalyst, solvent, monomer, nucleation, and workup activation, which have been shown as an effective means to expedite the formation of COFs. While promising, we foresee a number of limitations and challenges that need to be addressed in order to further advance the field of expeditious COF synthesis:

1) Most synthetic approaches have only been demonstrated for specific types of COFs, thus seriously restricting the scope of methodologies. For instance, mechanochemical and sonothermal syntheses are largely limited to *β*-ketoenamine-linked COFs and boron-based COFs, respectively. Furthermore, imine-linked COFs have been predominantly studied whereas the rapid synthesis of COFs bearing new linkages has been comparatively underexplored. Therefore, developing an uncomplicated and more general approach for the rapid synthesis of COFs with new linkages is greatly desired.
2) While some of the energy sources such as the planetary mill and electron accelerator are more attractive on the manufacturing scale, these may not be as accessible in research laboratories, thus constraining their broad utility.
3) The fundamental mechanism of COFs' expeditious formation is still not utterly understood. For instance, alternative energy sources such as mechanical agitation, light-irradiation, and electron beams, offer an efficient and eco-friendly route to the rapid synthesis of COFs. How does the nucleation and growth change during the synthesis? In-depth studies such as *in situ* kinetics analysis may cast light on the mechanism of COFs formation.
4) The rapid synthesis of COFs is presently limited to 2D COFs whereas minimal studies have been conducted in 3D COFs, except one ionothermal synthesis using ionic liquids. The expeditious synthesis of 3D COFs is worth more attention.[110]
5) Finally, the stability (e.g., chemical and mechanical) and scalable synthesis of COFs are both of great significance for their potential industrial practice and commercialization.[111, 112] Therefore, developing COFs with combined traits of pronounced stability, potential scalability, and expeditious formation is an appealing research direction worth earnest efforts.

Albeit these challenges, the development of rapid COF chemistry has been quite inspiring in providing a potentially more sustainable approach to porous materials with augmented properties and performances. More interdisciplinary and sustained efforts in the rapid construction of high-quality COFs will open up numerous possibilities for their further explorations.

Conflicts of interest

There are no conflicts of interest to declare.

Acknowledgements

We would like to thank the support from the Molecular Foundry, Lawrence Berkeley National Laboratory, a user facility supported by

the Office of Science, Office of Basic Energy Sciences, of the U.S. Department of Energy under contract no. DE-AC02-05CH11231. Y. Lv and Z. Chen also acknowledge the support of the National Key Research and Development Program of China (2018YFA0902200) and the National Natural Science Foundation of China (31961133004).

References

1. A. P. Cote, A. I. Benin, N. W. Ockwig, M. O'Keeffe, A. J. Matzger and O. M. Yaghi, *Science*, 2005, **310**, 1166-1170.
2. R. P. Bisbey and W. R. Dichtel, *ACS Cent. Sci.*, 2017, **3**, 533-543.
3. N. Huang, P. Wang and D. Jiang, *Nat. Rev. Mater.*, 2016, **1**, 1-19.
4. M. S. Lohse and T. Bein, *Adv. Funct. Mater.*, 2018, **28**, 1705553.
5. C. S. Diercks and O. M. Yaghi, *Science*, 2017, **355**, eaal1585.
6. S. L. Cai, W. G. Zhang, R. N. Zuckermann, Z. T. Li, X. Zhao and Y. Liu, *Adv. Mater.*, 2015, **27**, 5762-5770.
7. Y. Song, Q. Sun, B. Aguila and S. Ma, *Adv. Sci.*, 2019, **6**, 1801410.
8. S. J. Lyle, P. J. Waller and O. M. Yaghi, *Trends Chem.*, 2019, **1**, 172-184.
9. S. Kandambeth, K. Dey and R. Banerjee, *J. Am. Chem. Soc.*, 2019, **141**, 1807-1822.
10. T. Ma, E. A. Kapustin, S. X. Yin, L. Liang, Z. Zhou, J. Niu, L.-H. Li, Y. Wang, J. Su, J. Li, X. Wang, W. D. Wang, W. Wang, J. Sun and O. M. Yaghi, *Science*, 2018, **361**, 48-52.
11. B. J. Smith, A. C. Overholts, N. Hwang and W. R. Dichtel, *Chem.Comm.*, 2016, **52**, 3690-3693.
12. T. Sick, J. M. Rotter, S. Reuter, S. Kandambeth, N. N. Bach, M. Döblinger, J. Merz, T. Clark, T. B. Marder, T. Bein and D. D. Medina, *J. Am. Chem. Soc.*, 2019, **141**, 12570-12581.
13. Y. Chen, Z.-L. Shi, L. Wei, B. Zhou, J. Tan, H.-L. Zhou and Y.-B. Zhang, *J. Am. Chem. Soc.*, 2019, **141**, 3298-3303.
14. S. Cai, B. Sun, X. Li, Y. Yan, A. Navarro, A. Garzón-Ruiz, H. Mao, R. Chatterjee, J. Yano, C. Zhu, J. A. Reimer, S. Zheng, J. Fan, W. Zhang and Y. Liu, *ACS Appl. Mater. Interfaces*, 2020, **12**, 19054-19061.
15. Z. Wang, Q. Yu, Y. Huang, H. An, Y. Zhao, Y. Feng, X. Li, X. Shi, J. Liang, F. Pan, P. Cheng, Y. Chen, S. Ma and Z. Zhang, *ACS Cent. Sci.*, 2019, **5**, 1352-1359.
16. C. H. Feriante, S. Jhulki, A. M. Evans, R. R. Dasari, K. Slicker, W. R. Dichtel and S. R. Marder, *Adv. Mater.*, 1905776.
17. K. Geng, T. He, R. Liu, K. T. Tan, Z. Li, S. Tao, Y. Gong, Q. Jiang and D. Jiang, *Chem. Rev.*, 2020. 10.1021/acs.chemrev.9b00550
18. Y. Li, W. Chen, G. Xing, D. Jiang and L. Chen, *Chem. Soc. Rev.*, 2020, **49**, 2852-2868.
19. Z. Wang, S. Zhang, Y. Chen, Z. Zhang and S. Ma, *Chem. Soc. Rev.*, 2020, **49**, 708-735.
20. T. Sun, J. Xie, W. Guo, D.-S. Li and Q. Zhang, *Adv. Energy Mater.*, 2020, **10**, 1904199.
21. R. K. Sharma, P. Yadav, M. Yadav, R. Gupta, P. Rana, A. Srivastava, R. Zbořil, R. S. Varma, M. Antonietti and M. B. Gawande, *Mater. Horiz.*, 2020, **7**, 411-454.
22. B. J. Smith and W. R. Dichtel, *J. Am. Chem. Soc.*, 2014, **136**, 8783-8789.
23. H. Li, A. D. Chavez, H. Li, H. Li, W. R. Dichtel and J.-L. Bredas, *J. Am. Chem. Soc.*, 2017, **139**, 16310-16318.
24. B. T. Koo, R. F. Heden and P. Clancy, *Phys. Chem. Chem. Phys.*, 2017, **19**, 9745-9754.
25. Q. Gao, L. Bai, Y. Zeng, P. Wang, X. Zhang, R. Zou and Y. Zhao, *Chem. Eur. J.*, 2015, **21**, 16818-16822.
26. H. Wang, B. He, F. Liu, C. Stevens, M. Brady, S. Cai, C. Wang, T. Russell, T.-W. Tan and Y. Liu, *J. Mater. Chem. C*, 2017, **5**, 5090-5095.
27. Z. Miao, G. Liu, Y. Cui, Z. Liu, J. Li, F. Han, Y. Liu, X. Sun, X. Gong and Y. Zhai, *Angew. Chem. Int. Ed.*, 2019, **58**, 4906-4910.
28. Y. Zhai, G. Liu, F. Jin, Y. Zhang, X. Gong, Z. Miao, J. Li, M. Zhang, Y. Cui and L. Zhang, *Angew. Chem. Int. Ed.*, 2019, **58**, 17679-17683.
29. W. Kong, W. Jia, R. Wang, Y. Gong, C. Wang, P. Wu and J. Guo, *Chem.Comm.*, 2019, **55**, 75-78.
30. D. M. Fischbach, G. Rhoades, C. Espy, F. Goldberg and B. J. Smith, *Chem.Comm.*, 2019, **55**, 3594-3597.
31. S. Kuecken, J. Schmidt, L. Zhi and A. Thomas, *J. Mater. Chem. A*, 2015, **3**, 24422-24427.
32. K. Geng, T. He, R. Liu, S. Dalapati, K. T. Tan, Z. Li, S. Tao, Y. Gong, Q. Jiang and D. Jiang, *Chem. Rev.*, 2020, DOI: 10.1021/acs.chemrev.9b00550.
33. N. L. Campbell, R. Clowes, L. K. Ritchie and A. I. Cooper, *Chem. Mater.*, 2009, **21**, 204-206.
34. S.-T. Yang, J. Kim, H.-Y. Cho, S. Kim and W.-S. Ahn, *RSC Adv.*, 2012, **2**, 10179-10181.
35. B. P. Biswal, S. Chandra, S. Kandambeth, B. Lukose, T. Heine and R. Banerjee, *J. Am. Chem. Soc.*, 2013, **135**, 5328-5331.
36. S. Kim, C. Park, M. Lee, I. Song, J. Kim, M. Lee, J. Jung, Y. Kim, H. Lim and H. C. Choi, *Adv. Funct. Mater.*, 2017, **27**, 1700925.
37. M. Zhang, J. Chen, S. Zhang, X. Zhou, L. He, M. V. Sheridan, M. Yuan, M. Zhang, L. Chen, X. Dai, F. Ma, J. Wang, J. Hu, G. Wu, X. Kong, R. Zhou, T. E. Albrecht-Schmitt, Z. Chai and S. Wang, *J. Am. Chem. Soc.*, 2020, **142**, 9169-9174.
38. A. de la Hoz, A. Diaz-Ortiz and A. Moreno, *Chem. Soc. Rev.*, 2005, **34**, 164-178.
39. V. Polshettiwar and R. S. Varma, *Acc. Chem. Res.*, 2008, **41**, 629-639.
40. A. Mirzaei and G. Neri, *Sens. Actuators B Chem.*, 2016, **237**, 749-775.
41. Y. Li and W. Yang, *J. Membr. Sci.*, 2008, **316**, 3-17.
42. J. Klinowski, F. A. Almeida Paz, P. Silva and J. Rocha, *Dalton Trans.*, 2011, **40**, 321-330.
43. M. Dogru, A. Sonnauer, S. Zimdars, M. Döblinger, P. Knochel and T. Bein, *CrystEngComm*, 2013, **15**, 1500-1502.
44. H. Wei, S. Chai, N. Hu, Z. Yang, L. Wei and L. Wang, *Chem.Comm.*, 2015, **51**, 12178-12181.
45. W. Ji, Y.-S. Guo, H.-M. Xie, X. Wang, X. Jiang and D.-S. Guo, *J. Hazard. Mater.*, 2020, **397**, 122793.
46. B. Zhang, M. Wei, H. Mao, X. Pei, S. A. Alshmimri, J. A. Reimer and O. M. Yaghi, *J. Am. Chem. Soc.*, 2018, **140**, 12715-12719.
47. G. Das, T. Skorjanc, S. K. Sharma, F. Gándara, M. Lusi, D. S. Shankar Rao, S. Vimala, S. Krishna Prasad, J. Raya, D. S. Han, R. Jagannathan, J.-C. Olsen and A. Trabolsi, *J. Am. Chem. Soc.*, 2017, **139**, 9558-9565.
48. L. K. Ritchie, A. Trewin, A. Reguera-Galan, T. Hasell and A. Cooper, *Micropor. Mesopor. Mat.*, 2010, **132**, 132-136.
49. H. Xu, B. W. Zeiger and K. S. Suslick, *Chem. Soc. Rev.*, 2013, **42**, 2555-2567.
50. P. Zhang and S. Dai, *J. Mater. Chem. A*, 2017, **5**, 16118-16127.
51. M. E. Casco, S. Kirchhoff, D. Leistenschneider, M. Rauche, E. Brunner and L. Borchardt, *Nanoscale*, 2019, **11**, 4712-4718.
52. W. Xiao, S. Yang, P. Zhang, P. Li, P. Wu, M. Li, N. Chen, K. Jie, C. Huang, N. Zhang and S. Dai, *Chem. Mater.*, 2018, **30**, 2924-2929.
53. I.-Y. Jeon, H.-J. Choi, S.-M. Jung, J.-M. Seo, M.-J. Kim, L. Dai and J.-B. Baek, *J. Am. Chem. Soc.*, 2013, **135**, 1386-1393.

54. T. Stolar and K. Užarević, *CrystEngComm*, 2020, DOI: 10.1039/D0CE00091D.
55. S. Chandra, S. Kandambeth, B. P. Biswal, B. Lukose, S. M. Kunjir, M. Chaudhary, R. Babarao, T. Heine and R. Banerjee, *J. Am. Chem. Soc.*, 2013, **135**, 17853-17861.
56. G. Das, D. Balaji Shinde, S. Kandambeth, B. P. Biswal and R. Banerjee, *Chem.Comm.*, 2014, **50**, 12615-12618.
57. D. B. Shinde, H. B. Aiyappa, M. Bhadra, B. P. Biswal, P. Wadge, S. Kandambeth, B. Garai, T. Kundu, S. Kurungot and R. Banerjee, *J. Mater. Chem. A*, 2016, **4**, 2682-2690.
58. S. Karak, S. Kandambeth, B. P. Biswal, H. S. Sasmal, S. Kumar, P. Pachfule and R. Banerjee, *J. Am. Chem. Soc.*, 2017, **139**, 1856-1862.
59. B. Pietrobon and V. Kitaev, *Chem. Mater.*, 2008, **20**, 5186-5190.
60. L. Balan, M. C. Fernández de Córdoba, M. Zaier and C. O. Ania, *Carbon*, 2017, **116**, 264-274.
61. K. L. McGilvray, M. R. Decan, D. Wang and J. C. Scaiano, *J. Am. Chem. Soc.*, 2006, **128**, 15980-15981.
62. S. Kim and H. C. Choi, *Commun. Chem.*, 2019, **2**, 1-8.
63. Z. Meng, R. M. Stolz and K. A. Mirica, *J. Am. Chem. Soc.*, 2019, **141**, 11929-11937.
64. H. Fujita, M. Izawa and H. Yamazaki, *Nature*, 1962, **196**, 666-667.
65. Z. Xu, L. Chen, B. Zhou, Y. Li, B. Li, J. Niu, M. Shan, Q. Guo, Z. Wang and X. Qian, *RSC Adv.*, 2013, **3**, 10579-10597.
66. M. Zhang, Q. Gao, C. Yang, L. Pang, H. Wang, H. Li, R. Li, L. Xu, Z. Xing and J. Hu, *Ind. Eng. Chem. Res.*, 2016, **55**, 10523-10532.
67. M. Matsumoto, R. R. Dasari, W. Ji, C. H. Feriante, T. C. Parker, S. R. Marder and W. R. Dichtel, *J. Am. Chem. Soc.*, 2017, **139**, 4999-5002.
68. Rebecca L. Li, N. C. Flanders, A. M. Evans, W. Ji, I. Castano, L. X. Chen, N. C. Gianneschi and W. R. Dichtel, *Chem. Sci.*, 2019, **10**, 3796-3801.
69. M. Li, S. Qiao, Y. Zheng, Y. H. Andaloussi, X. Li, Z. Zhang, A. Li, P. Cheng, S. Ma and Y. Chen, *J. Am. Chem. Soc.*, 2020, **142**, 6675-6681.
70. H.-L. Qian, F.-L. Meng, C.-X. Yang and X.-P. Yan, *Angew. Chem. Int. Ed.*, 2020, 10.1002/anie.202006535
71. X. Guan, Y. Ma, H. Li, Y. Yusran, M. Xue, Q. Fang, Y. Yan, V. Valtchev and S. Qiu, *J. Am. Chem. Soc.*, 2018, **140**, 4494-4498.
72. J. Qiu, H. Wang, Y. Zhao, P. Guan, Z. Li, H. Zhang, H. Gao, S. Zhang and J. Wang, *Green Chem.*, 2020, **22**, 2605-2612.
73. M. Liu, L. Guo, S. Jin and B. Tan, *J. Mater. Chem. A*, 2019, **7**, 5153-5172.
74. K. Wang, L. M. Yang, X. Wang, L. Guo, G. Cheng, C. Zhang, S. Jin, B. Tan and A. Cooper, *Angew. Chem. Int. Ed.*, 2017, **56**, 14149-14153.
75. P. Kuhn, M. Antonietti and A. Thomas, *Angew. Chem. Int. Ed.*, 2008, **47**, 3450-3453.
76. J. Liu, W. Zan, K. Li, Y. Yang, F. Bu and Y. Xu, *J. Am. Chem. Soc.*, 2017, **139**, 11666-11669.
77. S. Y. Yu, J. Mahmood, H. J. Noh, J. M. Seo, S. M. Jung, S. H. Shin, Y. K. Im, I. Y. Jeon and J. B. Baek, *Angew. Chem. Int. Ed.*, 2018, **57**, 8438-8442.
78. Z. Yang, H. Chen, S. Wang, W. Guo, T. Wang, X. Suo, D.-e. Jiang, X. Zhu, I. Popovs and S. Dai, *J. Am. Chem. Soc.*, 2020, **142**, 6856-6860.
79. J. Tan, S. Namuangruk, W. Kong, N. Kungwan, J. Guo and C. Wang, *Angew. Chem. Int. Ed.*, 2016, **55**, 13979-13984.
80. X. Li, H. Wang, H. Chen, Q. Zheng, Q. Zhang, H. Mao, Y. Liu, S. Cai, B. Sun and C. Dun, *Chem*, 2020, **6**, 933-944.
81. M. Liu, Q. Huang, S. Wang, Z. Li, B. Li, S. Jin and B. Tan, *Angew. Chem. Int. Ed.*, 2018, **57**, 11968-11972.
82. L. Zhang, R. Liang, C. Hang, H. Wang, L. Sun, L. Xu, D. Liu, Z. Zhang, X. Zhang, F. Chang, S. Zhao and W. Huang, *Green Chem.*, 2020, **22**, 2498-2504.
83. C.-X. Yang, C. Liu, Y.-M. Cao and X.-P. Yan, *Chem.Comm.*, 2015, **51**, 12254-12257.
84. A. de la Peña Ruigómez, D. Rodríguez-San-Miguel, K. C. Stylianou, M. Cavallini, D. Gentili, F. Liscio, S. Milita, O. M. Roscioni , M. L. Ruiz-González, C. Carbonell, D. Maspoch, R. Mas-Ballesté, J. L. Segura and F. Zamora, *Chem. Eur. J.*, 2015, **21**, 10666-10670.
85. D. Rodríguez-San-Miguel, J. J. Corral-Pérez, E. Gil-González, D. Cuellas, J. Arauzo, V. M. Monsalvo, V. Carcelén and F. Zamora, *CrystEngComm*, 2017, **19**, 4872-4876.
86. S. Liu, C. Hu, Y. Liu, X. Zhao, M. Pang and J. Lin, *Chem. Eur. J.*, 2019, **25**, 4315-4319.
87. W. Ma, Q. Zheng, Y. He, G. Li, W. Guo, Z. Lin and L. Zhang, *J. Am. Chem. Soc.*, 2019, **141**, 18271-18277.
88. L. A. Blanchard, D. Hancu, E. J. Beckman and J. F. Brennecke, *Nature*, 1999, **399**, 28-29.
89. F. Zhang, J. Zhang, B. Zhang, X. Tan, D. Shao, J. Shi, D. Tan, L. Liu, J. Feng and B. Han, *ChemSusChem*, 2018, **11**, 3576-3580.
90. S.-Y. Ding, J. Gao, Q. Wang, Y. Zhang, W.-G. Song, C.-Y. Su and W. Wang, *J. Am. Chem. Soc.*, 2011, **133**, 19816-19822.
91. J. Thote, H. Barike Aiyappa, R. Rahul Kumar, S. Kandambeth, B. P. Biswal, D. Balaji Shinde, N. Chaki Roy and R. Banerjee, *IUCrJ*, 2016, **3**, 402-407.
92. D. Stewart, D. Antypov, M. S. Dyer, M. J. Pitcher, A. P. Katsoulidis, P. A. Chater, F. Blanc and M. Rosseinsky, *Nat. Commun.*, 2017, **8**, 1-10.
93. J. A. Martín, D. Rodríguez-San-Miguel, C. Franco, I. Imaz, D. Maspoch, J. Puigmartí-Luis and F. Zamora, *Chem.Comm.*, 2020, **56**, 6704-6707.
94. J. Lu, F. Lin, Q. Wen, Q.-Y. Qi, J.-Q. Xu and X. Zhao, *New J. Chem.*, 2019, **43**, 6116-6120.
95. Z. Kang, Y. Peng, Y. Qian, D. Yuan, M. A. Addicoat, T. Heine, Z. Hu, L. Tee, Z. Guo and D. Zhao, *Chem. Mater.*, 2016, **28**, 1277-1285.
96. Y. Liu, Y. Wang, H. Li, X. Guan, L. Zhu, M. Xue, Y. Yan, V. Valtchev, S. Qiu and Q. Fang, *Chem. Sci.*, 2019, **10**, 10815-10820.
97. Y. Zhao, L. Guo, F. Gándara, Y. Ma, Z. Liu, C. Zhu, H. Lyu, C. A. Trickett, E. A. Kapustin and O. Terasaki, *J. Am. Chem. Soc.*, 2017, **139**, 13166-13172.
98. Q. Guan, D.-D. Fu, Y.-A. Li, X.-M. Kong, Z.-Y. Wei, W.-Y. Li, S.-J. Zhang and Y.-B. Dong, *iScience*, 2019, **14**, 180-198.
99. Y. Li, Q. Chen, T. Xu, Z. Xie, J. Liu, X. Yu, S. Ma, T. Qin and L. Chen, *J. Am. Chem. Soc.*, 2019, **141**, 13822-13828.
100. F. J. Uribe-Romo, C. J. Doonan, H. Furukawa, K. Oisaki and O. M. Yaghi, *J. Am. Chem. Soc.*, 2011, **133**, 11478-11481.
101. G. Chen, H.-H. Lan, S.-L. Cai, B. Sun, X.-L. Li, Z.-H. He, S.-R. Zheng, J. Fan, Y. Liu and W.-G. Zhang, *ACS Appl. Mater. Interfaces*, 2019, **11**, 12830-12837.
102. X. Li, J. Qiao, S. W. Chee, H.-S. Xu, X. Zhao, H. S. Choi, W. Yu, S. Y. Quek, U. Mirsaidov and K. P. Loh, *J. Am. Chem. Soc.*, 2020, **142**, 4932-4943.
103. E. Vitaku and W. R. Dichtel, *J. Am. Chem. Soc.*, 2017, **139**, 12911-12914.
104. W. Zhao, J. Qiao, T.-L. Ning and X.-K. Liu, *Chinese J. Polym. Sci.*, 2018, **36**, 1-7.
105. M. D. Oleksiak, J. A. Soltis, M. T. Conato, R. L. Penn and J. D. Rimer, *Chem. Mater.*, 2016, **28**, 4906-4916.
106. M. J. Van Vleet, T. Weng, X. Li and J. R. Schmidt, *Chem. Rev.*, 2018, **118**, 3681-3721.

107. Y.-C. Yuan, B. Sun, A.-M. Cao, D. Wang and L.-J. Wan, *Chem.Comm.*, 2018, **54**, 5976-5979.
108. B. Sun, D. Wang and L. Wan, *Sci. China Chem.*, 2017, **60**, 1098-1102.
109. A. P. Nelson, O. K. Farha, K. L. Mulfort and J. T. Hupp, *J. Am. Chem. Soc.*, 2009, **131**, 458-460.
110. X. Ma and T. F. Scott, *Commun. Chem.*, 2018, **1**, 98.
111. W. Zhao, L. Xia and X. Liu, *CrystEngComm*, 2018, **20**, 1613-1634.
112. X. Li, C. Zhang, S. Cai, X. Lei, V. Altoe, F. Hong, J. J. Urban, J. Ciston, E. M. Chan and Y. Liu, *Nat. Commun.*, 2018, **9**, 2998.

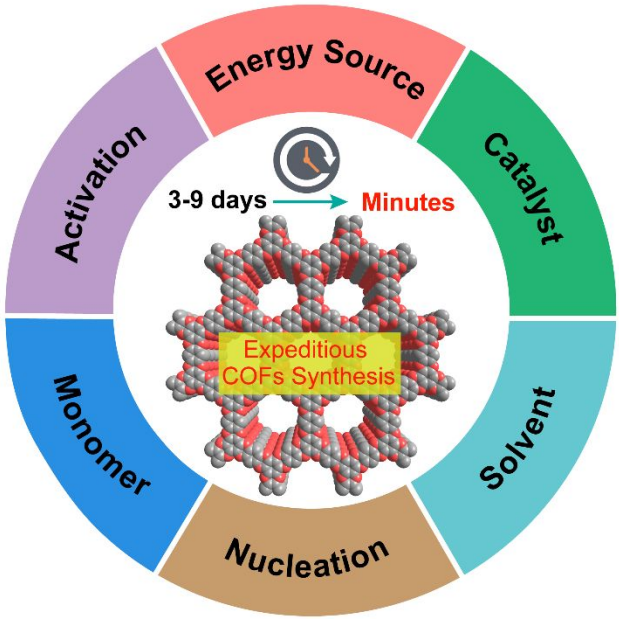

A comprehensive overview of the advances in the expeditious synthesis of COFs.